

Sintering and physicochemical properties of titania

Ibticem Ayadi ^{a,*} and Foued Ben Ayed ^a

^aLaboratory of Industrial Chemistry, National School of Engineering, Sfax University, Box 1173, 3038 Sfax, Tunisia.

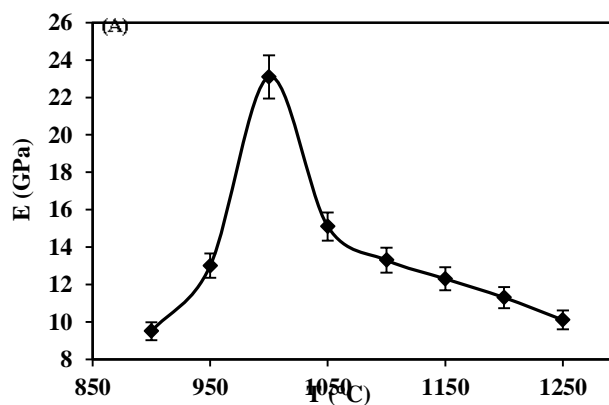
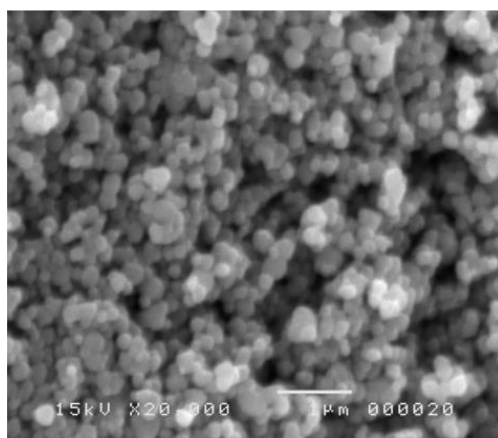
* Corresponding author E-Mail: ayadi.ibticem@gmail.com
Phone: 00 216 52 293 466, Fax: 00 216 74 275 595

- **Novelty and Highlights:**

1. Titania annealed 1000°C, exhibit better mechanical properties.
2. The anatase phase is totally transformed to rutile phase after the sintering process of titania at 1000°C for 300 minutes.

- **Graphical Abstract:**

Above 1000°C, the mechanical properties and the densification of titania are hindered by the allotropic transformation of titania.





Sintering and physicochemical properties of titania

Ibticem Ayadi ^{a,*} and Foued Ben Ayed ^a

^aLaboratory of Industrial Chemistry, National School of Engineering, Sfax University, Box 1173, 3038 Sfax, Tunisia.

* Corresponding author E-Mail: ayadi.ibticem@gmail.com

Phone: 00 216 52 293 466, Fax: 00 216 74 275 595

Abstract

The sintering behavior and the mechanical properties of titania have been investigated. The characterization of titania before and after the sintering process was realized by the differential thermal analysis, the dilatometry, the X-ray diffraction, the infrared spectroscopy and the scanning electron microscopy. The mechanical performances of titania increased with both the sintering temperature and the length of the sintering times. At 1000°C, the mechanical properties of titania reached their maximum value. Thus, the optimum value of the rupture strength reached 7MPa, whereas Vickers hardness attained 340 Hv; the shear modulus and Young's modulus registered optimum values: 10.5GPa and 23.1GPa, respectively. Above 1000°C, the mechanical properties and the densification of titania are hindered by the allotropic transformation of titania. Thus, the allotropic transformation of titania from anatase phase to rutile phase was totally achieved after the sintering process at 1000°C for 300 minutes.

Key words: Titania, annealing, mechanical properties, anatase, rutile phase.

Introduction

Nanocrystalline titania (TiO₂) in both powder and compact forms is an attractive material, applicable to various fields, such as biomedical applications, semiconductor, photocatalysts, photovoltaic and mesoporous membranes [1-16]. Titanium oxide has been studied recently thanks to their interesting physical, chemical and electrical properties. Titania has been widely studied due to its bioinertness, excellent tribological properties, high wear resistance, fracture toughness and strength as well as relatively low friction [3, 6-12]. Titania is considered as having excellent biocompatibility, manifested in various biomedical applications, such as orthopedic devices, maxillofacial surgery and dental implants [7, 14-15]. This work proposes to study the sintering behavior of titania at various sintering temperatures (between 900°C and 1250°C) for different length of the sintering times (between 0 min and 300 min). This study has allowed us to define the sintering temperature and the length of the sintering times for which titania should have an optimum values of densification and mechanical properties. In the present work, titania was characterized with the differential thermal analysis, the dilatometry, the X-Ray diffraction, the infrared spectroscopy, the density and the mechanical properties measurements such as: the rupture strength (σ_r), Vickers hardness (H) and the elastic modulus (E and G).

Experimental

The commercial titania (Fluka, purity = 99%) was used in this study. The powder of titania is molded in a cylinder having a 20 mm as diameter and a 6 mm as thickness and pressed under 150 MPa. The samples were sintered at various temperatures for different length of the sintering times in a vertical furnace (Pyrox 2408). The heating rate is 10°C min⁻¹. The size of the particles of the powder was measured by means of a Micromeritics Sedigraph 5000. The specific surface area (SSA) was measured using the BET (Brunauer–Emmett–Teller) method and using N₂ as an adsorption gas [17]. The primary size (D_{BET}) was calculated by assuming the primary particles to be spherical [18]:

$$D_{BET} = \frac{6}{S\rho} \quad (1)$$

Where ρ is the theoretical density and S is the specific surface area.

The powder is submitted to infrared spectrometry (FTIR) analysis (Perkin-Elmer 783). The powder was analyzed by using X-ray diffraction (XRD). The X-ray patterns were recorded using the Seifert XRD 3000 TT diffractometer. The X-ray radiance was produced by using CuK α radiation ($\lambda=1.54056\text{\AA}$). The crystalline phases were identified with the powder diffraction files (PDF) of the international Center for Diffraction Data (ICDD). The lattice parameters were refined by least-square calculation with reflections obtained from powder diffractograms (program DICVOL) [19].

The linear shrinkage was determined using dilatometry analysis (Setaram TMA 92 dilatometry). The heating and

cooling rates are $10^{\circ}\text{C min}^{-1}$ and $20^{\circ}\text{C min}^{-1}$, respectively. Differential thermal analysis (DTA) was carried out using about 30 mg of powder (DTA-TG, Setaram Model). The heating rate was $10^{\circ}\text{C min}^{-1}$.

The microstructure of the sintered compacts was investigated on samples of the fractured surfaces with a scanning electron microscope (SEM) (JSM-5400). These samples were coated with a gold layer for more electronic conductivity.

The Brazilian test was conducted to measure the rupture strength of titania [20-21]. The rupture strength (σ_r) values were measured using the Brazilian test according to the equation (2):

$$\sigma_r = \frac{2 \times P}{\Pi \times D \times t} \quad (2)$$

Where P being the maximum applied load, D being the diameter, t being the thickness of the disc and σ_r being the rupture strength (or mechanical strength).

Hardness of samples was measured by Vickers indentation using loading values of about 5 or 10 kg applied for 15 s. The surface of the samples was polished between $1 \mu\text{m}$ and $3 \mu\text{m}$ using diamond paste. Ten indentations were made for each measurement and hardness was calculated using equation (3) [22]:

$$H = 1.8544 (P/d^2) \quad (3)$$

Where H is the Vickers hardness, P is the indentation load and 'd' is the indent diagonal length. Average hardness value was taken from ten indentations made for each sample and the maximum error obtained was found to be less than 5%.

The testing instrument includes a high-frequency generator Model 5077PR (Olympus). The samples have been characterized and evaluated using the ultrasound techniques [23]. Young's modulus and the shear modulus were calculated from the point of the longitudinal and the transversal ultrasonic velocities [23].

Results

Characterization of titania powder

The experimental characteristics of titania powder are illustrated in Table 1 which summarizes the specific surface area (SSA), the average grain size obtained by different methods and theoretical density. The titania particles are assumed to be spherical; the particles size can be calculated using the equation (1). The average grain size obtained by the SSA (D_{BET}) and the granulometric repartition (D_{50}) are presented in Table 1. The value obtained by the SSA is similar to those obtained from the granulometric repartition (D_{50}) (Table 1).

The differential thermal analysis curve of titania shows one endothermic peak at 230°C (Figure 1a). This peak is followed by a small shoulder due a slight dehydroxylation of titania surface. The thermogravimetric analysis of titania indicates the dehydroxylation between 100°C and 400°C (Figure 1b). Thus, the weight loss is about 2.5% (Figure 1b). The dehydroxylation of titanium hydroxide into titania occurred the following reaction:



This result is similar to the previously reported in the literature [13].

Table 1. Characteristics of titania powder.

Compound	SSA(m ² /g)	D _{BET} (μm)	D ₅₀ ^a (μm)	d ^b (g/cm ³)
Anatase-TiO ₂	12	0.11	0.20	3.89

^aMean diameter, ^bTheoretical density.

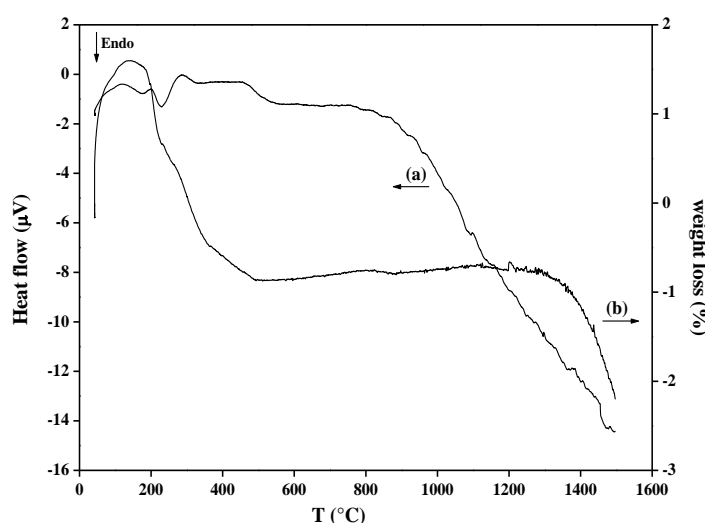


Figure 1. DTA and TG curves of titania powder.

The shrinkage curve of titania shows the phase transformation from anatase phase to rutile phase (Figure 2). Thus, the allotropic transformation of titania started at about 1090°C . The shrinkage curve shows also the sintering domain which began at 900°C and finished at 1100°C (Figure 2).

The sintering process and the mechanical properties of titania

The sintering of titania is examined between 900°C and 1250°C for 60 minutes. Figure 3a shows the typical relationship between the temperature and the density. A significant improvement of the density of titania was recorded with the increase in temperature up to 1000°C (Figure 3a). The optimum value of the density of titania is obtained after the sintering process at 1000°C for 60 minutes (73%) as shown in Figure 3a.

Beyond 1000°C , the densification was hindered and remains practically constant between 1050°C and 1250°C (Figure 3a). Figure 3b shows the rupture strength of titania sintered at various temperatures for 60 minutes. The results of sample's densification according to the sintering temperature are confirmed by the rupture strength study (Figure 3b) which shows a similar evolution. This curve illustrates the optimum value of the rupture strength obtained at 1000°C (5.7MPa) (Figure 3b).

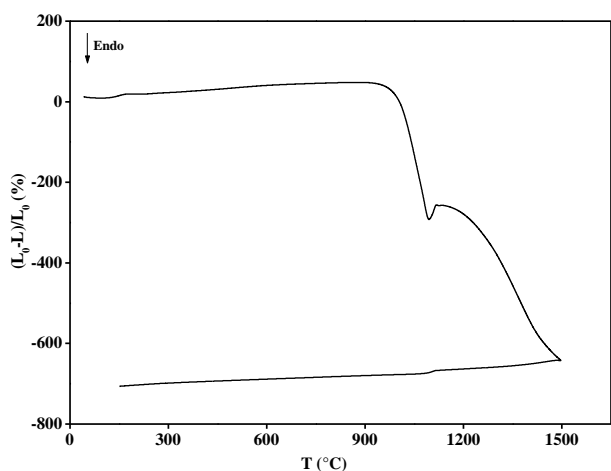


Figure 2. Linear shrinkage curve of titania.

Above 1000°C, the rupture strength decreases with the sintering temperature (Figure 3b). The results of the densification of titania are confirmed by the mechanical study. Thus, the optimum values are obtained after the sintering process at 1000°C for 60 minutes.

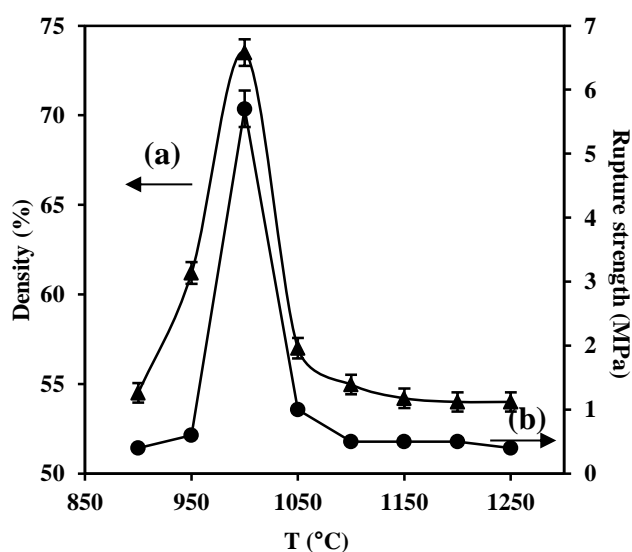


Figure 3. The density and the rupture strength of titania sintered for 60 minutes at various temperatures.

Figure 4a shows the densification results of titania sintered at 1000°C for different length of the sintering times (between 0 min and 300 min). The densification of titania increases with the length of the sintering times (Figure 4a). The ultimate densification was obtained by firing for 300 minutes at 1000°C (75%). Figure 4b shows the rupture strength of titania sintered at 1000°C for different length of the sintering times. The evolution of mechanical properties of titania was considered as a function of the length of the sintering times. The maximum of the rupture strength reached 7 MPa at 1000°C for 300 minutes (Figure 4b).

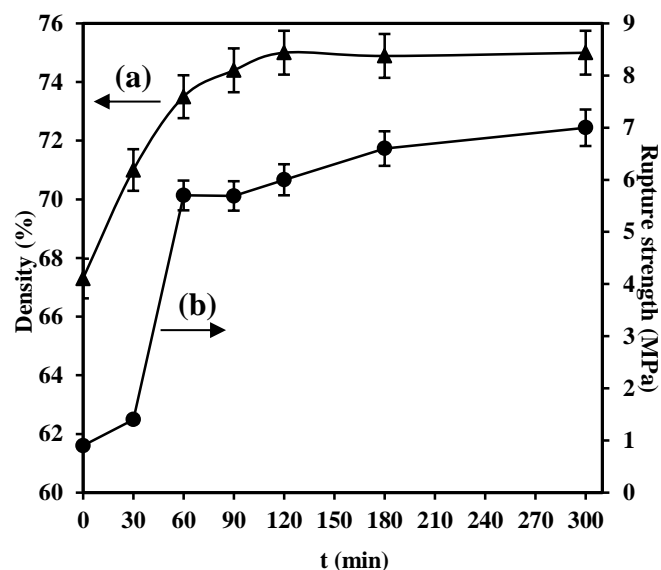


Figure 4. The density and the rupture strength of titania sintered at 1000°C for different length of the sintering times.

The influence of the sintering temperature on Vickers hardness (H) of the samples is shown in Figure 5. Vickers hardness of titania is studied at various temperatures for 60 minutes. Vickers hardness of titania rapidly increases from 31.5 to 340 Hv when the sintering temperature increases from 900°C to 1000°C. Consequently, Vickers hardness of titania reached its maximum value (340 Hv) at 1000°C for 60 minutes (Figure 5). Above 1000°C, Vickers hardness brutally decreases to 300 Hv. The hardness evolution of the sintered titania is so close to the evolution of the density and the rupture strength.

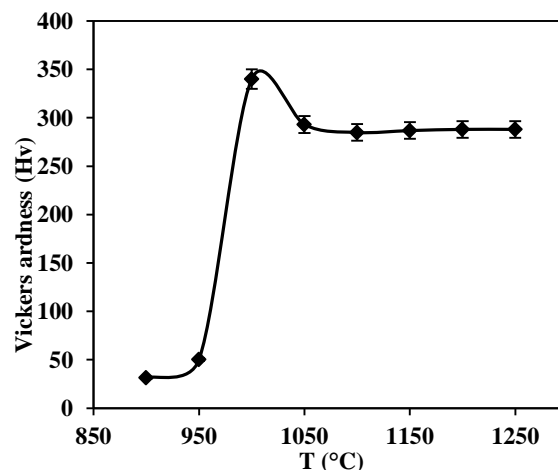


Figure 5. Vickers hardness of titania sintered for 60 minutes at various temperatures.

The variation of Vickers hardness of titania sintered at 1000°C with different length of the sintering times is shown

in Figure 6. Thus, Vickers hardness of titania increased with the length of the sintering times and reached its maximum value (340 Hv) after 60 minutes. Above 60 minutes, Vickers hardness decreases with the length of the sintering times. Vickers hardness of titania increases after the sintering process at 1000°C for 300 minutes. This result was explained by the formation of rutile phase of titania which is responsible for the better Vickers hardness (330 Hv) at this conditions.

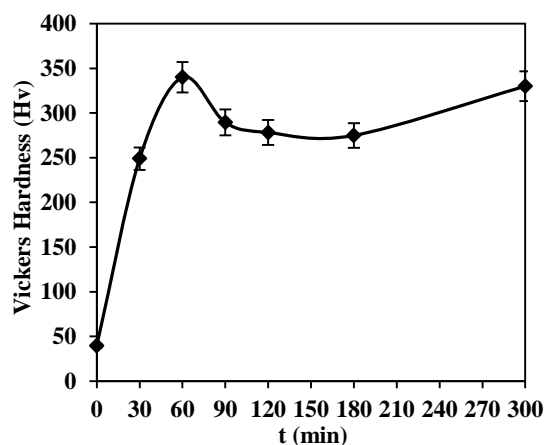


Figure 6. Vickers hardness of titania sintered at 1000°C for different length of the sintering times.

Figure 7 shows the evolution of Young's modulus (E) and the shear modulus (G) of titania sintered at various temperatures for 60 minutes. Both of the elastic modulus (E and G) of titania reached optimum values at 1000°C (E = 23.1 GPa, G = 10.5 GPa). Above 1000°C, the mechanical performances of samples rapidly decreased with sintering temperature (Figure 7). The variation of the elastic modulus of titania sintered at 1000°C for different length of the sintering times are shown in Figure 8. The optimum values of E and G are obtained once again at 1000°C for 60 minutes. Above 90 minutes, the elastic modulus of titania increases after the sintering process at 1000°C for 180 minutes and 300 minutes. The same evolution of the elastic modulus of titania was detected for Vickers hardness (Figures 6 and 8). Thus, the presence of rutile phase of titania has given better mechanical properties of titania at this condition (above 90 minutes and at 1000°C).

Characterization of titania after the sintering process

The characterization of titania was realized by the X-Ray diffraction (XRD), the infrared spectroscopy (FTIR) and the scanning electronic microscopy (SEM).

The XRD spectra of titania sintered at various temperatures for 60 minutes are shown in Figure 9. All the diffraction peaks correspond to anatase phase of titania (Figure 9). When the specimens are sintered at 1000°C, we have seen low intensity peaks of titania rutile phase (Figure 9b).

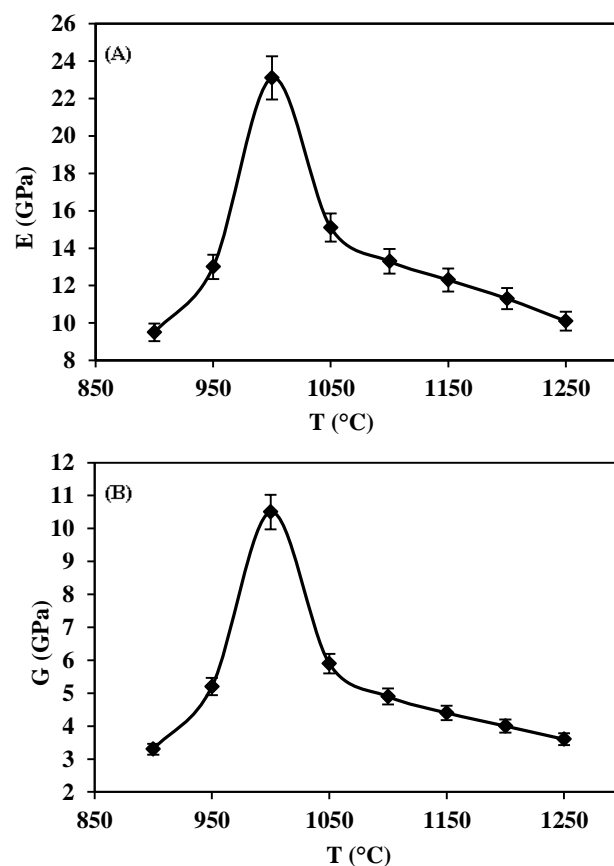


Figure 7. (A) Young's modulus of titania sintered at various temperatures for 60 minutes. (B) Shear modulus of titania sintered at various temperatures for 60 minutes.

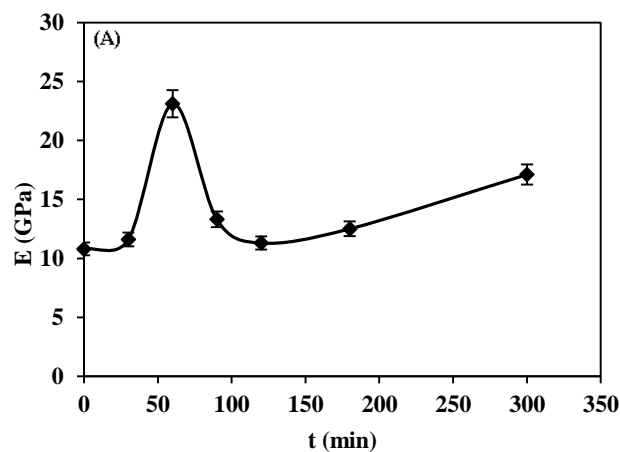


Figure 8. (A) Young's modulus of titania sintered at 1000°C for different length of the sintering times.

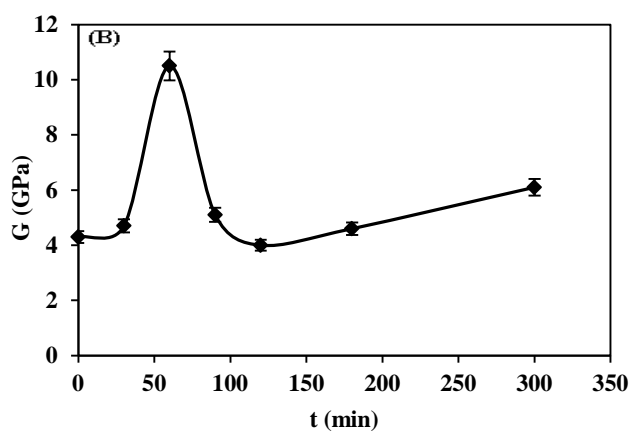


Figure 8. (B) Shear modulus of titania sintered at 1000°C for different length of the sintering times.

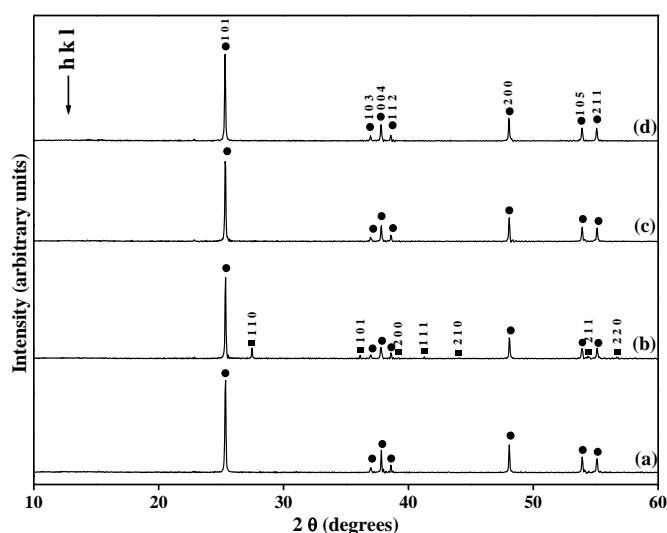


Figure 9. XRD spectra of titania sintered for 60 minutes at: (a) 900°C, (b) 1000°C, (c) 1100°C and (d) 1200°C. (●: anatase, ■ : rutile).

The XRD spectra of titania sintered at 1000°C for different sintering times are reported in Figure 10. The XRD spectra of titania sintered at 1000°C for 0 minutes shows only the anatase phase (Figure 10a). The titania rutile traces are obtained at 1000°C for 60 minutes (Figure 10b). The peaks intensity of rutile phase of titania increase with the length of the sintering times (Figure 10b-10d). Thus, the transformation of titania from anatase to rutile is completely achieved after the sintering process at 1000°C for 300 minutes (Figure 10d).

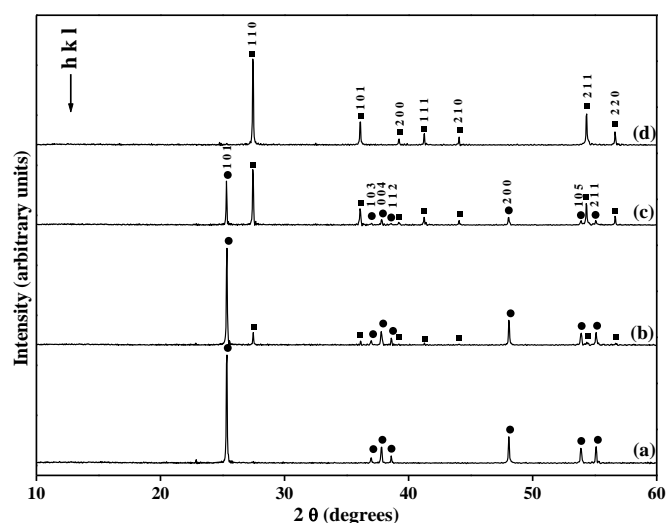


Figure 10. XRD spectra of titania sintered at 1000°C for different sintering times: (a) 0 min, (b) 60 min, (c) 180 min and (d) 300 min. (●: anatase, ■ : rutile).

Table 2 shows the crystalline parameters of titania sintered at various temperatures for different length of the sintering times. The crystalline parameters of titania correspond to anatase phase when the samples sintered at 1100°C and 1200°C for 60 minutes (Table 2). Thus, the crystalline parameters of titania (sintered at 1100°C and 1200°C) are similar to the theoretical values of the anatase phase (Table 2). After the sintering process of the samples at 1000°C for 300 minutes, the crystalline parameters correspond to rutile phase (Table 2). The X-Ray diffraction analysis was conducted to analyse the transformation from anatase to rutile phase. This transformation was characterized by the variation of the crystalline parameters of titania after the sintering process (Table 2). The anatase phase is totally transformed to rutile phase after the sintering process of titania at 1000°C for 300 minutes (Table 2) and (Figure 10d).

Infrared spectra of TiO₂ sintered for 60 minutes at various temperatures (900°C, 1000°C, 1100°C, and 1200°C) indicate the presence of characteristics bands of titania (Figure 11A). In practically, the bands at 697 cm⁻¹ and 547 cm⁻¹ are characteristics of anatase phase of titania (Figure 11). These peaks are attributed to Ti–O bond. Thus, the band at 697 cm⁻¹ refers to symmetric O–Ti–O stretch while 547 cm⁻¹ is due to the vibration of Ti–O bond. The infrared spectroscopy of titania sintered at 1000°C for different length of the sintering times is illustrated in Figure 11B. This Figure shows further the bands of anatase phase and the presence of a new band at 415 cm⁻¹ corresponding to rutile phase of titania (Figure 11B (c-d)). Thus, the results of the infrared spectroscopy of titania confirms those of the X-Ray diffraction.

After the sintering process, the characteristics of the samples were investigated using the scanning electronic microscopy.

Table 2. Crystalline parameters of titania after the sintering process.

T (°C) / t(min)	Anatase	Rutile
1000°C/60min	a = b = 12.6671 Å c = 11.8889 Å V* = 1907.64 Å ³	-
1100°C/60min	a = b = 3.7840 Å c = 9.5135 Å V = 136.22 Å ³	-
1200°C/60min	a = b = 3.7853 Å c = 9.5151 Å V = 136.34 Å ³	-
1000°C/300min	-	a = b = 4.5911 Å c = 2.9578 Å V = 62.34 Å ³
Theoretical values [34]	a = b = 3.7842 Å c = 9.5146 Å V = 136.25 Å ³	a = b = 4.5845 Å c = 2.9533 Å V = 62.07 Å ³

Figure 12 shows the microstructure of titania (fracture surfaces) sintered at various temperatures (900°C, 1000°C, 1100°C and 1200°C) for different length of the sintering times. At 900°C, the sample presents an important intergranular porosity (Figure 12a). The grains size is around 0.2 μm. At 1000°C, the intergranular porosity is partially eliminated due to the grain growth (Figure 12a-b). The continuous phases increased with the sintering temperature (Figure 12a-b). Thus, titania particles went through the stages of partial coalescence (at 1000°C) (Figure 12b). At 1100°C and 1200°C, the microstructure of titania presents the growth of grains and the presence of opened and closed pores (Figure 12e-f). The microstructure of titania sintered at 1000°C for 300 minutes reveals the influence of the length of the sintering time (Figure 12c-d). The scanning electronic microscopy observations showed continuous phases (Figure 12c-d). The titania particles went through stages of completely coalescence (Figure 12c-d). A dense biomaterial was clearly formed: dense contacts between the grains and the well-formed grain boundary zone (Figure 12c-d).

Discussion

Pure titanium and titanium alloys are frequently used as dental and orthopedic implants, facial treatment and surgical instruments due to their excellent mechanical strength, biocompatibility and chemical stability outstanding properties [3-16]. Titania is chemically stable and is applied widely in various fields [6-8, 11, 13-16]. For this reason, we have chosen to study the sintering and the mechanical properties of titania.

The obtained results show that titania present excellent performances after the sintering process at 1000°C for 300 minutes. In fact, the densification reached 75% and the mechanical strength was about 7MPa. Table 3 shows examples from the literature of the mechanical properties of some bioceramics and the bone tissues. We notice the

similarity between the present work and the literature. Thus, the rupture strength of titania (7 MPa) is close to the enamel, higher than some bioceramics (β-TCP, ZrO₂) and smaller than alumina [24-30].

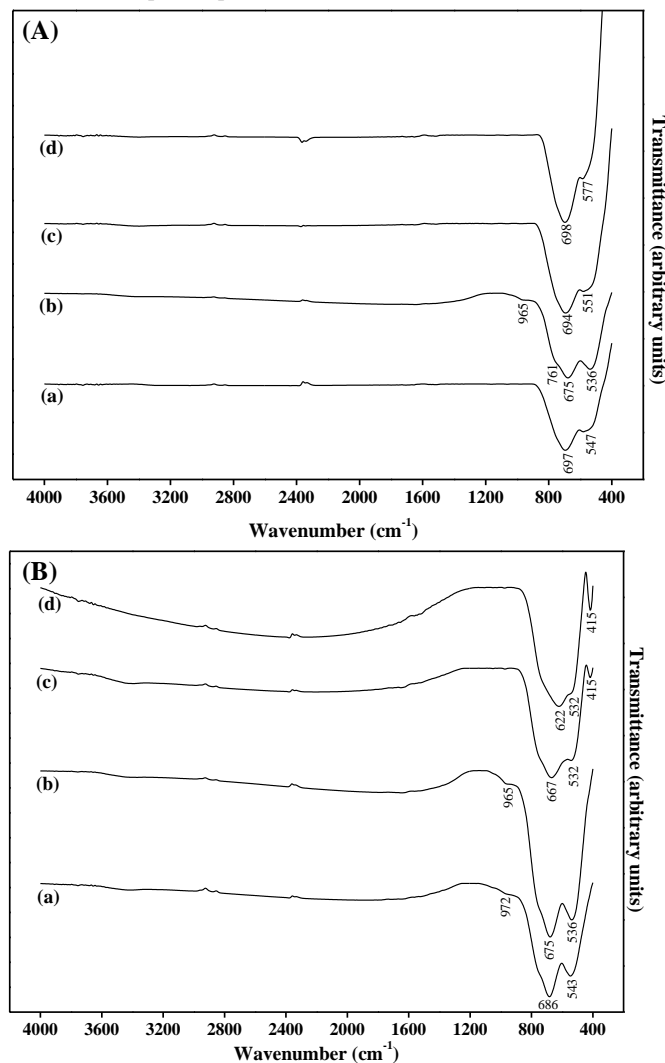


Figure 11. (A) Infrared spectra of titania sintered for 60 minutes at: (a) 900°C, (b) 1000°C, (c) 1100°C and (d) 1200°C. (B) Infrared spectra of titania sintered at 1000°C for different sintering times: (a) 0 min, (b) 60 min, (c) 180 min and (d) 300 min.

The hardness of titania reached its maximum value (340 Hv) after the sintering process at 1000°C for 60 minutes. This result was previously confirmed by the literature [9]. Thus, Qiu *et al.* indicate that the average hardness of TiO₂ produced by sol-gel synthesis process was only 317 Hv [9].

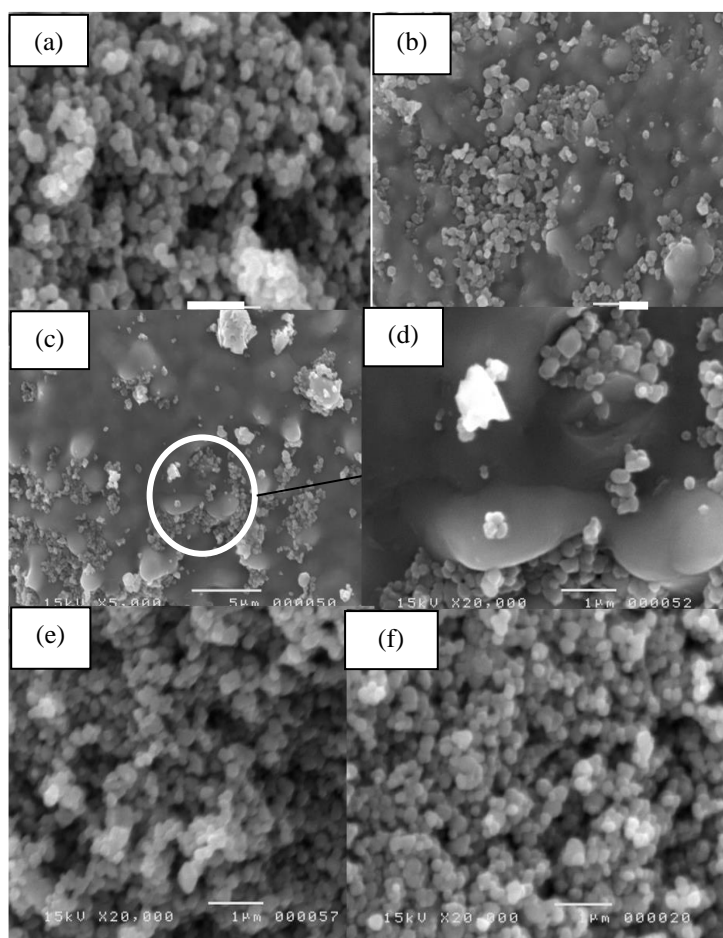


Figure 12. SEM micrograph (fracture) of titania sintered at: (a) 900°C, 60 min; (b) 1000°C, 60 min; (c) 1000°C, 300 min; (d) 1000°C, 300 min; (e) 1100°C, 60 min and (f) 1200°C, 60 min.

In the other hand, the obtained hardness (340 Hv) was similar to the enamel (340 Hv-370 Hv) [24-25, 33]. The optimal value of Young modulus of titania (23.1GPa) was so close to those of the cortical bone [24, 31-33]. In summary, the mechanical properties of the titania are more closely comparable to those bone tissues (Table 3). Thus, this result reveals the importance of titania in the biomedical applications [24-25, 31-33].

We have characterized the resulting titania after the sintering process with the mechanical properties, the density and the physicochemical characterization such as the X-Ray diffraction, the infrared spectroscopy, the dilatometry and the DTA-TG. The X-ray diffraction spectra of titania sintered at various temperatures for 60 minutes indicate the presence of the anatase phase and low peaks of rutile phase. The peaks intensity of rutile phase increase with the length of the sintering times (Table 2). Thus, the allotropic transformation of titania from anatase phase to rutile phase was totally achieved after the sintering process at 1000°C for 300 minutes. The same phenomenon was observed in the

literature [4, 11-12]. In fact, Mazaheri *et al.* show the similar results during the study of the sintering of titania assisted by anatase-to-rutile phase transformation [11, 12]. The results of infrared analysis of titania confirm those obtained by the X-Ray diffraction. In fact, the infrared spectra of titania sintered at 1000°C for 300 minutes show the characteristics bands of anatase phase and the presence of a new band at 415cm⁻¹ which is relative to the rutile phase. Thus, these results are similar to those obtained by previous works conducted by several researches [1-4].

Table 3. Examples from of the mechanical properties of some bioceramics and the bone tissues.

Materials	σ_r^a (MPa)	G^b (GPa)	E^c (GPa)	H^d (Hv)	References
β -TCP	4-6	7	17.5	-	[26-30]
Al_2O_3	10	-	-	-	[28]
ZrO_2	5	-	-	-	[27]
Enamel	8-12	-	82	340-370	[24-25, 33]
Cortical bone	-	-	7-25	-	[24, 31-32]
Dentin	-	-	18	40-75	[25, 31-32]
TiO_2	7	10.5	23.1	340	Present work

Conclusion

In this study, we examine the influence of the sintering temperatures and the length of the sintering times on the performances of titania such as the density, the rupture strength, the elastic modulus (E and G) and Vickers hardness. The sintering of titania indicates the evolution of the densification, the microstructure and the mechanical properties. In fact, the mechanical performances of titania increased with both the sintering temperatures and the length of the sintering times. Titania sintered at 1000°C for 300 minutes exhibit both high densification (75%) and better rupture strength ($\sigma_r = 7$ MPa). The optimum values of mechanical properties of titania (H = 340 Hv, E = 23.1 GPa and G = 10.5 GPa) obtained after the sintering process at 1000°C for 60 minutes. Above 1000°C, the densification and the mechanical performances of the samples were hindered by the allotropic transformation from anatase phase to rutile phase of titania. This allotropic transformation is achieved completely after the sintering process at 1000°C for 300 minutes.

References

- [1] M. Ocaña, V. Fornés, J.V. García Ramos and C.J. Serna, *J. Sol. State. Chem.*, 1988, **75**, 364-372.



- [2] H.M. Kim, F.Miyaji, T.Kokubo and T.Nakamura, *J. Biomed. Mater. Res.*, 1996, **32**, 409-417.
- [3] S. Musić, M. Gotić, M. Ivanda, S. Popović, A. Turković, R. Trojko, A. Sekulić and K. Furić, *Mater. Sci. Eng.*, 1997, **B47**, 33-40.
- [4] P.I. Gouma and M.J. Mills, *J. Am. Ceram. Soc.*, 2001, **84**, 619-622.
- [5] H. Kaneko, M. Uchida, T. Kokubo and T. Nakamura, *Key. Eng. Mater., Trans. Tech. Publications.*, Switzerland, 2002, pp. 649-652.
- [6] M. Maeda and T. Watanabe, *Thin Sol. Film.*, 2005, **489**, 320-324.
- [7] R. Carbone, I. Marangi, A. Zanardi, L. Giorgetti, E. Chierici, G. Berlanda, A. Podestà, F. Fiorentini, G. Bongiorno, P. Piseri, P.G. Pelicci and P. Milani, *Biomater.* 2006, **27**, 3221-3229.
- [8] C.K. Shin, Y.K. Paek and H.J. Lee, *Inter. J. Appl. Ceram. Technol.*, 2006, **3**, 463-469.
- [9] S. Qiu and S.J. Kalita, *Mater. Sci. Eng.*, 2006, **A 435-436**, 327-332.
- [10] D. Li, S. Chen, Y. Jing, W. Shao, Y. Zhang and W. Luan, *Sci. Sinter.*, 2007, **39**, 103-110.
- [11] M. Mazaheri, Z.R. Hesabi and S.K. Sadrnezhaad, *Scr. Mater.*, 2008, **59**, 139-142.
- [12] M. Mazaheri, A.M. Zahedi, M. Haghghatzadeh and S.K. Sadrnezhaad, *Ceram. Int.*, 2009, **35**, 685-691.
- [13] X. Miao, D. Sun and P.W. Hoo, *Ceram. Int.*, 2009, **35**, 281-288.
- [14] S. Jung and J.H. Kim, *Kor. J. Chem. Eng.*, 2010, **27(2)**, 645-650.
- [15] N.E. Mojtaba, E.K. Reza, M.S. Dadash and S. Karbasi, *Curr. Nanosci.*, 2011, **7**, 568-575.
- [16] I. Ayadi and F. Ben Ayed, *J. Mech. Behav. Biomed.*, 2015, **49**, 129-140.
- [17] S. Brunauer, P.H. Emmet and J. Teller, *J. Am. Chem. Soc.*, 1938, **60**, 310-319.
- [18] D. Bernache-Assollant, *Hermès science publications, Lavoisier*, 1993.
- [19] D.E. Appleman and H.T. Evans Jr, Job 9214: "Indexing and least-squares refinement of powder diffraction data" U.S. Geological Survey Computer Contribution 20 (NTIS Document PB2-16188. 1973) "CELREF", J. Laugieret A. Filhol 1978.
- [20] ISRM. *Int. J. Rock.Mech. Min. Sci. Geomech. Abstr.*, 1978, **15**, 99-103.
- [21] ASTM C496, Standard test method for splitting tensile strength of cylindrical concrete specimens Annual Book of ASTM, Standards, col. 0.042, ASTM, Philadelphia, 1984.
- [22] ASTM C1327-96, Standard test method for Vicker's indentation hardness of advanced ceramics. In: Annual book of ASTM standards, 2003, vol. 15.01.
- [23] Y. Chevalier, *Tech. Ingén. Reference AM5401*, 2003, pp. 1-19.
- [24] L.L. Hench, *J Wilson ed. Vol. 1.*, World Scientific, Singapore, 1993.
- [25] J.C. Elliott, *Elsevier Science B.V.*, Amsterdam, 1994.
- [26] N. Bouslama, F. Ben Ayed and J. Bouaziz, *Ceram. Int.*, 2009, **35**, 1909-1917.
- [27] I. Sallemi, F. Ben Ayed and J. Bouaziz, *Mater. Sci. Eng.*, 2012, **Vol. 28 (1)**, 012029.
- [28] S. Sakka, F. Ben Ayed and J. Bouaziz, *Mater. Sci. Eng.*, 2012, **Vol. 28 (1)**, 012028.
- [29] I. Sallemi, J. Bouaziz and F. Ben Ayed, *Mater. Chem. Phys.*, 2015, **151**, 50-59.
- [30] N. Bouslama, Y. Chevalier, J. Bouaziz and F. Ben Ayed, *Mater. Chem. Phys.*, 2013, **141**, 289-297.
- [31] A. Ravaglioli and A. Krajewski, *Chapman et Hall, London*, 1992, pp 422.
- [32] D. Shi, *Biomaterials and tissue engineering, Springer Berlin Heidelberg*, New York, 2004.
- [33] K.J. Chun, H.H. Choi and J.Y. Lee, *J. Dent. Biomech.* 2014, **5**, 1-6.
- [34] C.J. Howard, T. M. Sabine and F. Dickson, *Acta. Cryst.*, 1992, **47**, 462-468.